

This is an electronic reprint of the original article. This reprint may differ from the original in pagination and typographic detail.

Catalytic synthesis of terpenoid-derived hexahydro-2H-chromenes with analgesic activity over halloysite nanotubes

Sidorenko, A. Yu; Kurban, Yu M.; Il'ina, I. V.; Li-Zhulanov, N. S.; Korchagina, D. V.; Ardashov, O. V.; Wörnå, J.; Volcho, K. P.; Salakhutdinov, N. F.; Murzin, D. Yu; Agabekov, V. E.

Published in:

Applied Catalysis A: General

DOI:

[10.1016/j.apcata.2021.118144](https://doi.org/10.1016/j.apcata.2021.118144)

Published: 25/05/2021

Document Version

Accepted author manuscript

Document License

CC BY-NC-ND

[Link to publication](#)

Please cite the original version:

Sidorenko, A. Y., Kurban, Y. M., Il'ina, I. V., Li-Zhulanov, N. S., Korchagina, D. V., Ardashov, O. V., Wörnå, J., Volcho, K. P., Salakhutdinov, N. F., Murzin, D. Y., & Agabekov, V. E. (2021). Catalytic synthesis of terpenoid-derived hexahydro-2H-chromenes with analgesic activity over halloysite nanotubes. *Applied Catalysis A: General*, 618, Article 118144. <https://doi.org/10.1016/j.apcata.2021.118144>

General rights

Copyright and moral rights for the publications made accessible in the public portal are retained by the authors and/or other copyright owners and it is a condition of accessing publications that users recognise and abide by the legal requirements associated with these rights.

Take down policy

If you believe that this document breaches copyright please contact us providing details, and we will remove access to the work immediately and investigate your claim.

Catalytic synthesis of terpenoid-derived hexahydro-2*H*-chromenes with analgesic activity over halloysite nanotubes

A.Yu. Sidorenko^{a*}, Yu.M. Kurban^a, I.V. Il'ina^b, N.S. Li-Zhulanov^b, D.V. Korchagina^b,
O.V. Ardashov^b, J. Wärnå^c, K.P. Volcho^b, N.F. Salakhutdinov^b, D.Yu. Murzin^{c*}, V.E. Agabekov^a

^aInstitute of Chemistry of New Materials of National Academy of Sciences of Belarus, 220141, Skaryna str, 36, Minsk, Belarus

^bNovosibirsk Institute of Organic Chemistry, Lavrentjev av. 9, 630090, Novosibirsk, Russian Federation

^cÅbo Akademi University, Biskopsgatan 8, 20500 Turku/Åbo, Finland

Corresponding authors

Dr. A.Yu. Sidorenko

e-mail: Sidorenko@ichnm.by;

Tel: +375 17 268 63 08

Address: Institute of Chemistry of New Materials of National Academy of Sciences of Belarus, 220141, Skaryna str, 36, Minsk, Belarus

Professor Dr. D.Yu. Murzin

Åbo Akademi University

Biskopsgatan 8, 20500, Turku/Åbo, Finland

Tel: + 358 2 215 4985

e-mail: dmitry.murzin@abo.fi

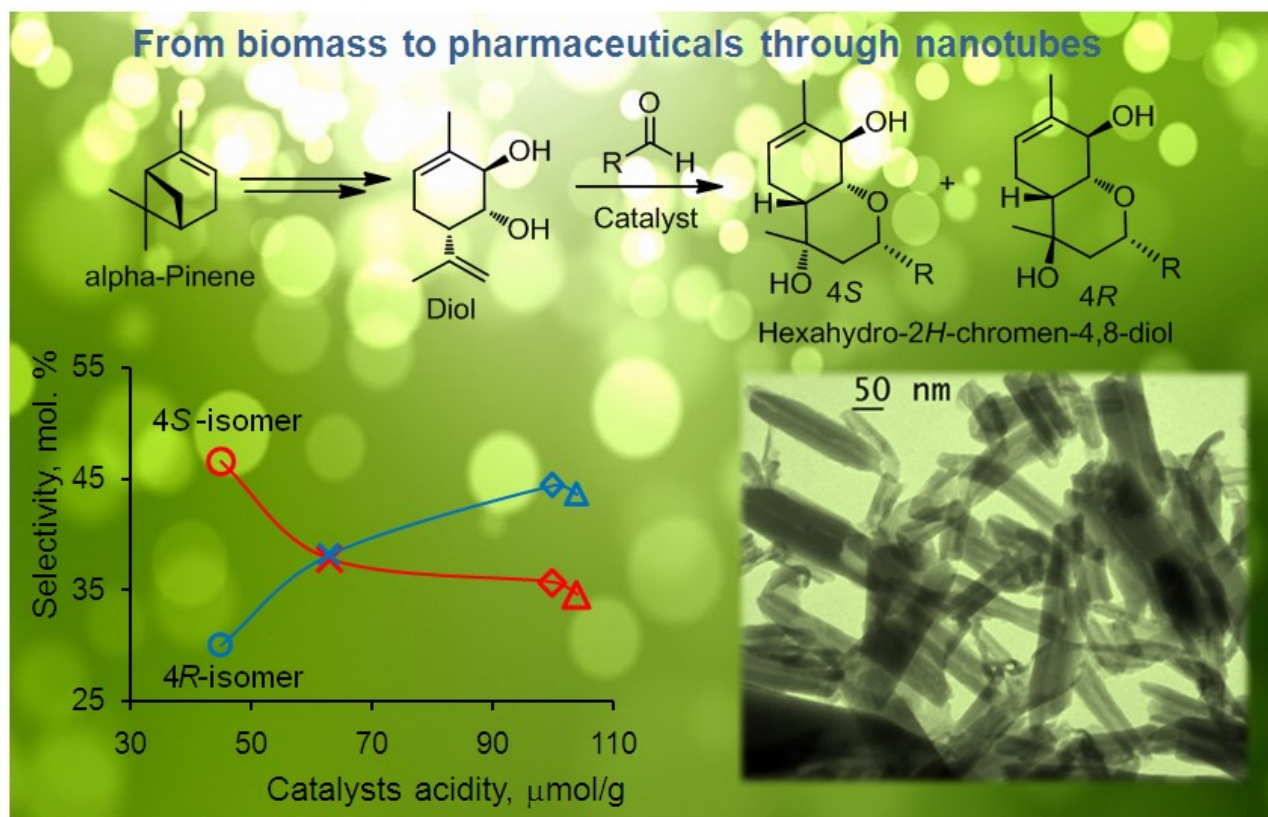
Abstract

Condensation of α -pinene derived *p*-menta-1,8-diene-5,6-diol (diol) with decanal was studied for the first time over modified halloysite nanotubes (HNT). The yield of the desired hexahydro-2*H*-chromene-4,8-diol with analgesic activity was 76–80% practically not depending on the catalyst type, while selectivity to 4*S*-isomer decreased, and to 4*R*-isomer increased with increasing acidity. The highest selectivity to 4*S*-diastereomer (48.1%) on halloysite is a result of weak acidity of this catalyst. DFT optimization of the key intermediate structure shows that the nucleophile attack proceeds at the equatorial position with the 4*S*-diastereomer formation, which was preferred on halloysite. On strong Brønsted (Amberlyst-15) and Lewis (scandium triflate) acids the target product yield did not exceed 37% because of dehydration. Halloysite nanocatalysts displayed a stable performance. In the case of diol reaction with a set of carbonyl compounds, the yields of hexahydro-2*H*-chromene-4,8-diols and the ratio of its 4*S*/4*R* isomers were significantly higher than on other catalysts.

Keywords

Terpenoids, halloysite, 2*H*-chromenes, acidity, Prins reaction, DFT

Graphical abstract



Highlights

- First systematic study of catalytic α -pinene derived diol condensation with an aldehydes to bioactive hexahydro-2H-chromene-4,8-diols.
- Halloysite nanocatalyst increases both the yields of hexahydro-2H-chromene-4,8-diols and 4S/4R isomers ratio.
- Inversion of stereoselectivity with increasing acidity or catalyst drying temperature.
- The reaction mechanism is discussed with DFT calculations and kinetic modeling.

1. Introduction

Many terpene hydrocarbons and terpenoids exhibiting various biological activities, are used in medical practice, and are promising for the development of new drugs [1–8]. Thus, medicines obtained from terpenoids are used in the treatment of infectious, oncological, skin and a number of other diseases [3, 4, 7, 8].

One of the most widespread in nature and available monoterpene hydrocarbons is α -pinene [9], on the basis of which the chiral monoterpene *p*-menta-1,8-diene-5,6-diol **1** was synthesized (Fig. 1a) [10]. It was found that diol **1** is highly active against symptoms of the Parkinson's disease [11] and is an extremely promising platform for the development of a new generation of antiparkinsonian drugs [12].

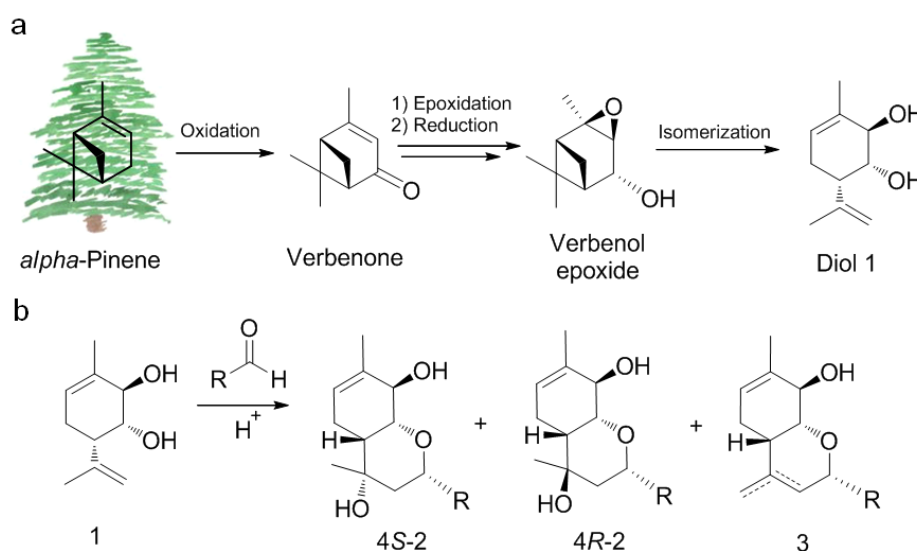


Fig. 1. Scheme for the diol synthesis (a) and its condensation with aldehydes (b)

From diol **1** a number of heterocyclic compounds promising for pharmaceutical application were also obtained [13]. Over acidic catalysts the diol can undergo condensation with aldehydes (Fig. 1b) to form substituted hexahydro-2*H*-chromene-4,8-diols **2** (as 4*S*- and 4*R*-diastereoisomers), as well as dehydration products **3** [14, 15]. It has been shown that a number of compounds with the structure **2**, which contain aromatic and aliphatic moieties, exhibit pronounced analgesic or antiviral

activity [13, 14]. For example, the diol **1** reaction with decanal on a commercial clay K-10 (Germany) leads to formation of the corresponding hexahydro-2*H*-chromene-4,8-diol (60%, 4*R*/4*S* ratio of 1:1), the analgesic effect of which was comparable to that for the reference drug diclofenac sodium [16].

It should be noted that the diol **1** reaction with carbonyl compounds over K-10 clay, as a rule, proceeds with relatively low (30–70%) total yields of hexahydrochromenols **2** [13]. When saturated aliphatic aldehydes were used as reagents, the formation of approximately equal amounts of 4*S*- and 4*R*-stereoisomers was observed [16], whereas in the case of unsaturated compounds or substituted benzaldehydes containing hydroxy and methoxy groups, the 4*S*-isomers were dominant in the product mixture [14, 16].

It is known that the biological activity of terpenoid derivatives can strongly depend on their configuration [11, 13]. For example, only one diastereomer of isopulegol derived chromene showed a high antiviral activity while another one was inactive [17]. Moreover, significant differences in the analgesic effects were demonstrated for chromenols obtained in the reaction of diol **1** with isovanillin but not with vanillin *per se* [18]. Subsequently, for an in-depth study of biological activity of this type of compounds, individual stereoisomers should be obtained. At the same, separation of such stereoisomers is usually a non-trivial task; therefore, development of stereoselective methods for synthesis of chromenol stereoisomers is important.

As catalysts for the monoterpenoid alcohols condensation with carbonyl compounds, modified clays [16–21], zeolites and mesoporous silicates [15, 22] SO₃H-functionalized carbon nanotubes [23], iodine [24], as well as traditional Lewis and Brønsted acids can be used [25–27].

In recent years, considerable attention of researchers has been attracted by the clay mineral halloysite, which morphologically represents multilayer nanotubes [28–31] consisting of tetrahedral Si–O and octahedral Al–O layers (Fig. 2). This natural nanomaterial, for example, can be used to create biomedical products and nanocomposites [29, 30], effective adsorbents of pollutants and heterogeneous catalysts [28 – 33].

For example, halloysite nanotubes (HNT) after their functionalization can be used as catalysts for various transformations, for example, Suzuki and Heck [34, 35], Fischer-Tropsch reactions [36], and for the conversion of carbohydrates to 5-hydroxymethylfurfural [37].

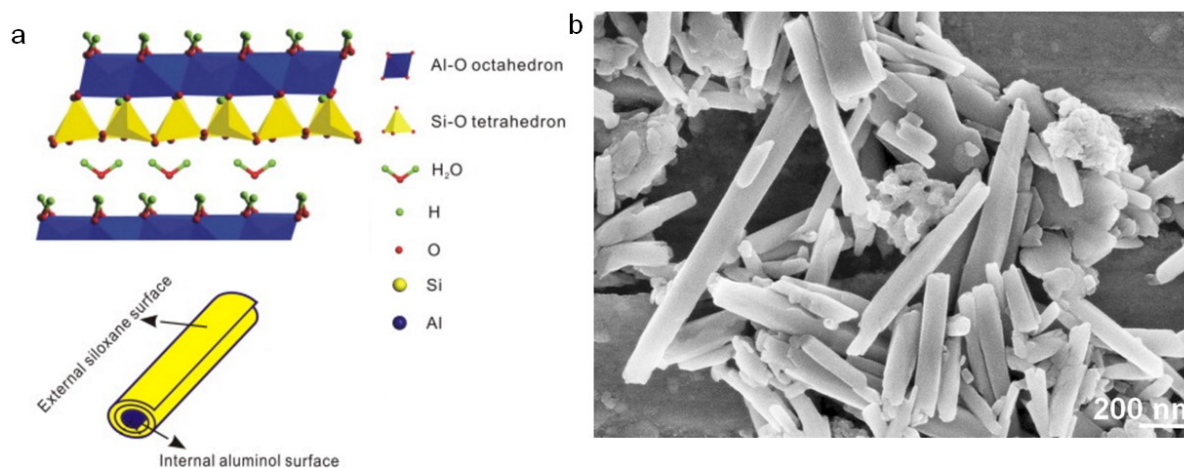


Fig. 2. Schematic structure (a) and SEM image (b) of halloysite (modified from [29, 38])

Recently, we have initiated utilization of halloysite nanotubes as catalysts for (-)-isopulegol **6** (Fig. 3) [38, 39] and (+)-2-carene [40] condensation with carbonyl compounds. It was shown that not only in the presence such catalysts selectivity to chiral octahydrochromenols (up to 90%) and isobenzofurans (up to 70%) significantly exceeded performance of other types of catalysts, but moreover HNT were stable and can be regenerated [38–40]. Thus, halloysite is a promising catalyst for the synthesis of heterocyclic compounds based on monoterpenoids.

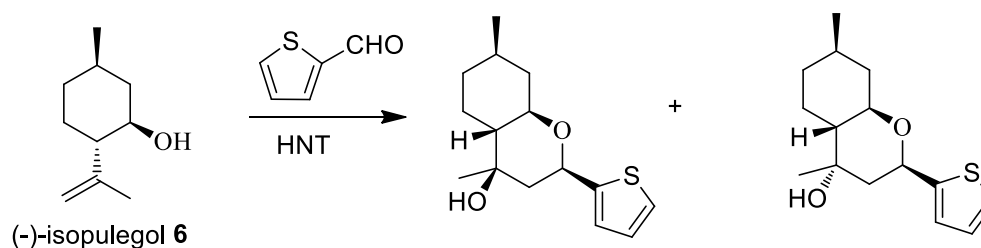


Fig. 3. Condensation of (-)-isopulegol with thiophene-2-carbaldehyde (modified from [38]).

Unlike isopulegol **6**, diol **1** contains additionally a hydroxyl group and a double bond which substantially affect its reactivity. Indeed, vicinal diols as well as allylic hydroxyls usually differ from aliphatic alcohols in chemical properties. Thus, it is not surprising that complex mixtures of products are often formed when the compound **1** reacts with aldehydes in the presence of K-10 clay significantly influencing resinification [41]. Usually, the reactions with diol **1** require longer time in comparison with isopulegol **6** and lead to lower yields of the desired products. Subsequently, development of new effective catalysts for reactions of diol **1** with carbonyl compounds is a timely and challenging task.

In this work, condensation of a set of monoterpene alcohols (diol stereoisomers **1** and **4**, and, for comparison, isopulegol **6** and neoisopulegol **8**) with carbonyl compounds on acid-modified halloysite nanotubes was studied. The main attention was paid to the reaction of diol **1** with decanal, since the resulting substituted hexahydro-2*H*-chromene-4,8-diol **2** has a high analgesic activity.

2. Experimental

All commercially available materials and reagents (purity at least 98%) were purchased from Sigma-Aldrich. Diol stereoisomers **1** and **4** were synthesized from (-)-verbenone and (+)- α -pinene correspondently in accordance with [11]. Neoisopulegol **8** was obtained from isopulegol **6** as described in [42].

2.1. Preparation of catalysts

Commercial halloysite (Sigma-Aldrich) from the Dragon Mine, USA, was used as a starting material for catalyst preparation. Acid treatment of HNT was carried out according to the following method [38]. In a three-necked (50 ml), equipped with a reflux condenser and a thermometer, a weighed portion of halloysite (7–9 g) was added and a 5% aqueous solution of HCl was added at the rate of 5 ml of acid per 1 g of solid (5 ml/g). The mixture was heated to 90°C and stirred (300 rpm) at this temperature for 3 h. Then the halloysite was washed until the absence of Cl⁻ ions in the wash

waters. The resulting solid phase was dried at 105°C to a constant weight, ground, and held for at least 72 h to obtain an air-dry form of the catalyst.

Commercial acid-modified montmorillonites K-10 and K-30 (Germany), illite clay (Russia), as well as strong Lewis (scandium triflate) and Brønsted (Amberlyst-15) acids were used for comparison. Illite clay was treated in a manner similar to HNT using 10% HCl solution [38]. The parent and modified halloysite was characterized by XRD, EDX, MAS NMR, SEM, TEM, FTIR with pyridine, thermogravimetry, and N₂ adsorption methods [38]. The physicochemical characteristics of K-10, K-30 and illite were studied in detail in [43]. The chemical composition, the porous structure parameters and acidity for the studied aluminosilicate materials are given in the Tables 1 and 2. In addition, the methodology for the acidity analyzing by the FTIR with pyridine is described in Supplementary information.

Table 1. Chemical composition and porous structure of the investigated solids

Catalyst	Oxide content, wt.%								Porous structure		
	Al ₂ O ₃	SiO ₂	FeO	Na ₂ O	MgO	K ₂ O	CaO	TiO ₂	S _{BET} , m ² /g	V _{pore} , cm ³ /g	d _{pore} , nm
Halloysite Initial* treated by 5% HCl*	44.1	54.4	0.5	0.2	0.1	-	0.4	0.3	60	0.22	15.7
	39.9	59.2	0.4	0.1	0.1	-	0.1	0.3	129	0.34	11.3
Illite*	19.8	64.4	6.4	0.1	1.7	5.6	0.1	1.9	146	0.28	8.1
K-10**	14.5	77.1	4.0	0.1	2.0	1.2	0.4	0.7	247	0.36	5.1
K-30**	13.1	81.2	3.4	0.1	1.4	1.1	0.2	0.5	339	0.51	5.4

The data from *[38] and **[43]

Table 2. Acidic properties of the investigated solids

Catalyst	Acid site concentration by FTIR with pyridine*, μmol/g							W/(M+S)	L/B
	Brønsted (B)			Lewis (L)			Total		
	Weak (W)	Medium (M)	Strong (S)	Weak (W)	Medium (M)	Strong (S)			
Halloysite Initial* treated by 5% HCl*	12	1	0	17	4	0	34	5.8	1.6
	12	3	0	19	6	5	45	2.2	2.0

Illite**	15	19	3	19	7	0	63	1.2	0.7
K-10***	15	26	7	35	14	7	104	0.9	1.2
K-30***	17	17	8	28	24	6	100	0.8	1.4

The data from *[38], **[40], and ***[43]

The treatment of halloysite nanotubes with 5% HCl led to an increase in its specific surface area from 60 to 129 m²/g (Table 1) and the acid sites (a.s.) concentration from 34 to 45 μmol/g (Table 2). In this case, the shape and size of the HNT did not change, and mainly the amorphous SiO₂ formation was observed at the ends of the nanotubes (Fig. 4) by breaking of Si–O–Al bonds and subsequent cross-linking of Si–OH fragments [38]. All investigated aluminosilicate materials are mesoporous (Table 1). **Note that the treatment of halloysite with 5% HCl did not change its XRD pattern, whereas, according to ²⁹Si MAS NMR, the content of amorphous SiO₂ was 15% [38].**

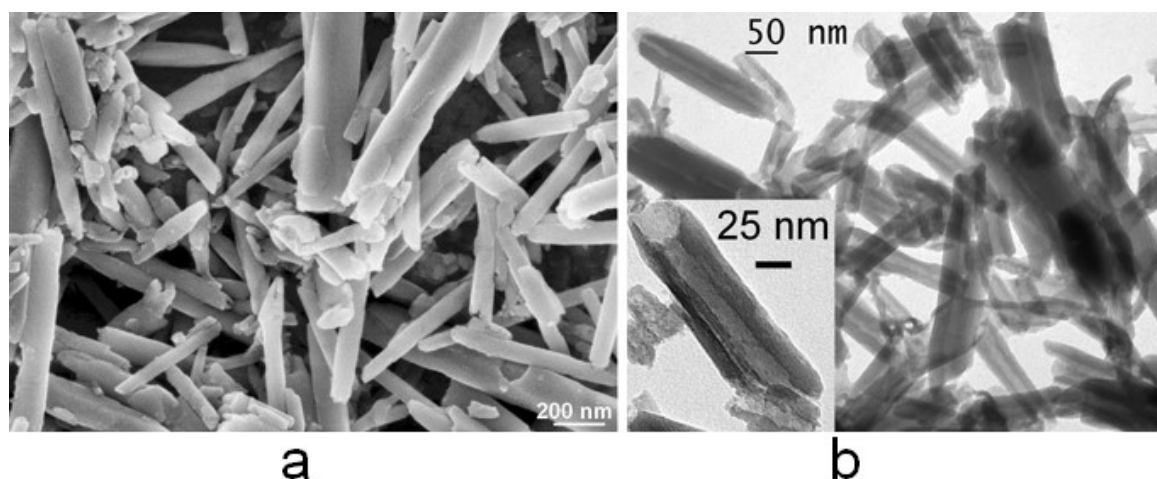


Fig. 4. SEM (a) and TEM images of halloysite treated with 5% HCl (modified from [34])

2.2. Reaction and analysis of products

A typical catalytic experiment was performed as follows. In a three-necked flask (25 ml) equipped with a temperature controller, a reflux condenser and a mechanical stirrer, 0.3 g (1.68 mmol) of diol **1**, an equivalent amount of decanal and dried toluene were added. The total volume of the mixture was 5 ml. After reaching the desired reaction temperature (40°C), the catalyst (0.56 g) was added and stirring was started (600 rpm). Samples of the reaction mixture were periodically

taken, being, after adding ethyl acetate, vigorous shaking, and separation of the catalyst, were analyzed by GC. Some experiments on the diol **1** condensation with a number of carbonyl compounds were carried out at room temperature without solvent according to the methods described in the [16].

The composition of the reaction mixture was determined using a Chromos GKh-1000 gas chromatograph with a flame ionization detector and a Zebron ZB-5 capillary column (30m x 0.25mm x 0.25 μ m). The evaporator and temperature detector temperature was 250 and 280 $^{\circ}$ C respectively. Heating of the column from 110 to 280 $^{\circ}$ C was done with the ramp of 20 $^{\circ}$ C/min, followed by the isothermal mode at 280 $^{\circ}$ C. The total analysis time was 30 min.

Separation of the reaction mixtures was performed by column chromatography. The structures of the obtained compounds were established by 1 H and 13 C NMR spectroscopy. Detailed techniques for products isolating and analysis are shown in Supplementary Information (SI).

The density functional theory (DFT) study was performed with the Jaguar 9.9 program using the dispersion-corrected hybrid density functional technique B3LYP-D3 with a 6-31G** basis set for structural geometry optimization [44]. The geometry optimizations were carried out in the gas-phase and the minima were confirmed by frequency calculations. Sample calculations using larger basis sets and other density functionals did not lead to significantly different geometries or energies.

3. Results and Discussion

3.1. Influence of catalysts type, acidity and thermal treatment

Taking into account that in Prins reaction the selectivity to tetrahydropyran alcohols increases with the addition of water or with the decrease in the catalyst drying temperature [38, 45, 46], the diol **1** condensation with decanal was initially carried out in the presence of air dry clays. **Note that preliminary experiments showed that the initial halloysite was practically not active in this reaction.**

In the presence of all investigated catalysts, the reaction products were substituted hexahydro-2H-chromene-4,8-diol **2** (as 4*S*- and 4*R*-diastereoisomers), as well as dehydration products **3** (Fig. 5).

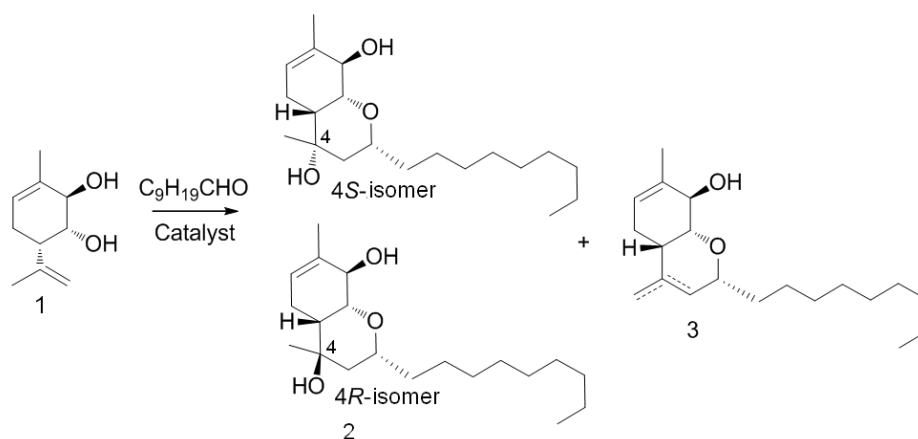


Fig. 5. A scheme of diol **1** condensation with decanal

At 70% conversion of diol **1** the total selectivity towards hexahydro-2*H*-chromene-4,8-diol **2** over studied catalysts was approximately the same (76–80%), whereas selectivity to its 4*S*- and 4*R*-isomers strongly depended on the catalyst type (Table 3). Thus, on halloysite nanotubes 4*S*-**2** compound prevailed in the reaction products (48.1%), while almost equal amounts of isomers were observed on illite clay. In the presence of montmorillonites K-10 and K-30, the main reaction product was the 4*R*-isomer (44.0%). The formation of dehydration products **3** on the investigated catalysts occurred in much smaller amounts (20.0–24.0%, Table 3).

It should be noted that the highest initial rate of consumption of diol **1** was observed in the presence of montmorillonite K-10, which is characterized by the highest concentration of acid sites (Table 3).

Table 3. Selectivity in the Prins reaction of diol **1*** with decanal at 40°C on various catalysts

Catalyst**	Acidity, $\mu\text{mol/g}$	r_0 , $\text{mmol/L}\cdot\text{g}\cdot\text{min}$	Time, min	Selectivity, mol. %				4 <i>S</i> /4 <i>R</i>
				2	4 <i>S</i> - 2	4 <i>R</i> - 2	3	
Halloysite	45	5.6	240	77.3	48.1	29.2	22.7	1.6
Illite	63	4.8	360	76.0	37.8	38.2	24.0	1.0
K-10	104	11.0	180	78.2	34.6	43.6	21.8	0.8
K-30	100	3.6	300	80.2	35.7	44.4	20.0	0.8

*At 70% conversion; **In air-dry state

To explain different stereoselectivity over the studied catalysts, the dependences of the yield of hexahydro-2*H*-chromene-4,8-diol **2** isomers on the concentration and strength of acid sites in the solids were analyzed.

The yield of 4*S*-**2** sharply decreases, while the yield of 4*R*-**2** increased with increasing of catalyst acidity (Fig. 6a). Therefore, a strong decrease in the 4*S*/4*R* ratio was also observed (Fig. 6b). Formation of the largest amount of 4*S*-**2** isomer (48.1%) was favored a low concentration of a.s. in the halloysite nanotubes (45 $\mu\text{mol/g}$). Application of montmorillonites K-10 and K-30 with higher acidity (up to 104 $\mu\text{mol/g}$) leads to inversion of stereoselectivity and predominance of the 4*R*-isomer (Fig. 6a).

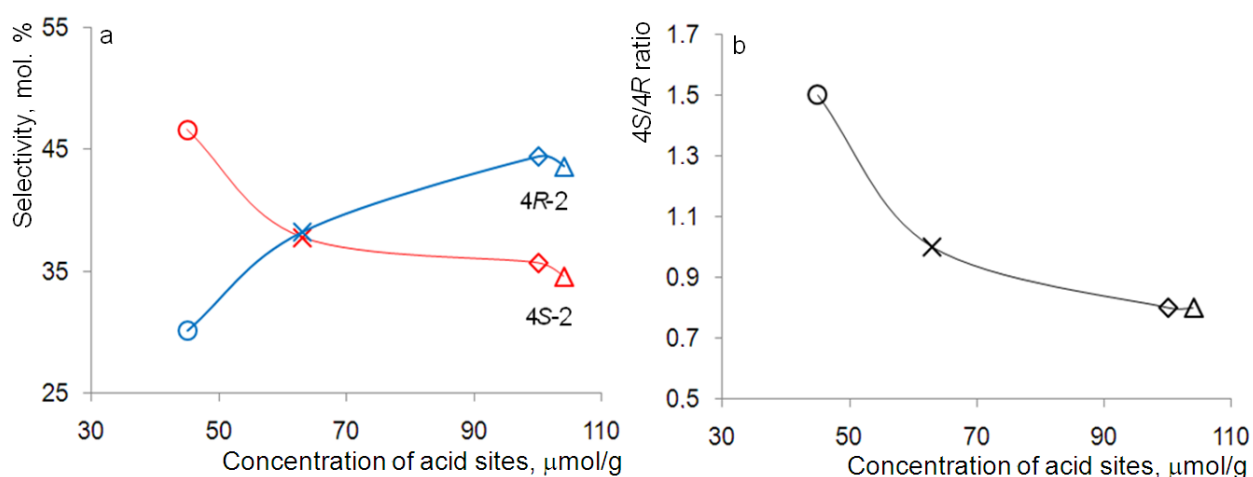


Fig. 6. Selectivity to hexahydro-2*H*-chromene-4,8-diol isomers (a) and 4*S*/4*R* ratio (b) as a function of catalyst acidity at 70% of diol conversion (\circ – HNT; X – illite; Δ – K-10; \diamond – K-30)

Stereoselectivity also depends on the strength of acid sites in the studied clays. Selectivity to the 4*S*-isomer increased with an increase in the number of weak (W) to the sum of medium (M) and strong (S) acid sites ratio, while the opposite dependence was obviously observed for the 4*R*-diastereomer (Fig. 7a). In this case, the 4*S*/4*R* ratio also increased (Fig. 7b). Thus, the most selective formation of the 4*S*-isomer of hexahydro-2*H*-chromene-4,8-diol **2** occurs on the weak acid sites on the catalyst surface.

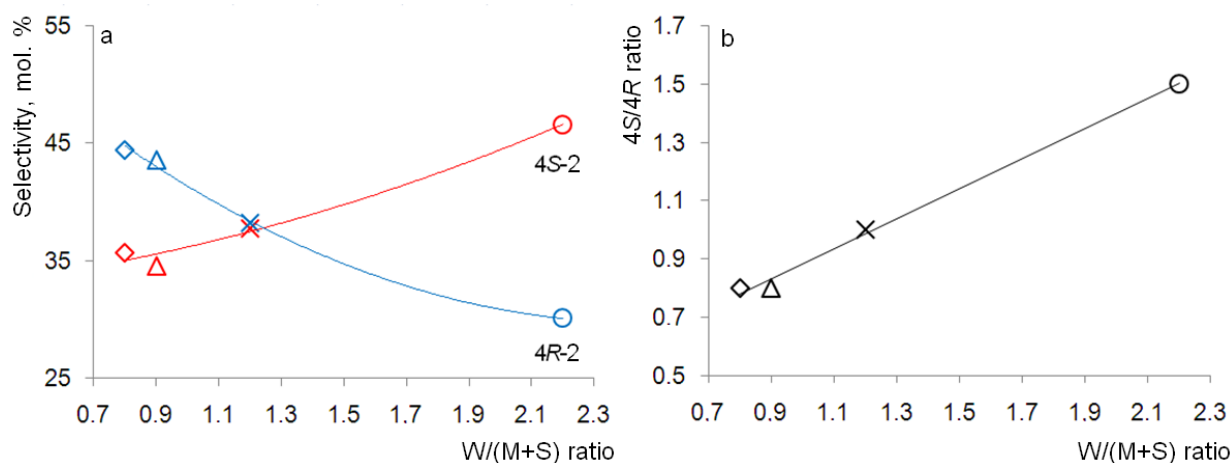


Fig. 7. Selectivity to hexahydro-2*H*-chromene-4,8-diol isomers (a) and 4*S*/4*R* ratio (b) as a function of the ratio between weak and the sum of medium and strong acid sites at 70% conversion of diol **1** (○– HNT; X – illite; Δ – K-10; ◇ – K-30)

The 4*S*/4*R* isomers ratio also can be influenced by their isomerization on the studied catalysts. To evaluate this phenomenon, dependences of selectivity to 4*S*- and 4*R*-diastereomers on the reaction time were analyzed (Fig. S1). It turned out that selectivity to these isomers practically did not change during the reaction, which clearly indicates absence of any significant effect of isomerization on the 4*S*/4*R* ratio. On this basis, acidity of the catalysts is considered as a key parameter for controlling stereoselectivity. The selectivity dependences on the diol conversion for halloysite are given below (Fig.8).

It should be noted that in a similar reaction of (-)-isopulegol with carbonyl compounds over various catalysts (clays, zeolites, iodine, scandium triflate), formation of predominantly 4*R*-diastereomers of octahydro-2*H*-chromene-4-ols was observed [19, 22, 24, 25, 38], i.e. isomers with *cis* arrangement of the substituents in the tetrahydropyran ring (Fig. S2). Moreover, selectivity for these isomers increased with a decrease in the concentration of acid sites, however, no inversion of stereoselectivity was observed [38, 39]. In the case of unsaturated aliphatic alcohols cyclization with aldehydes, *cis*-isomers of resulting tetrahydropyrans are also predominantly formed [45, 46]. Interestingly, that selectivity to *cis*-isomer practically did not depend on acidity of the clays used as catalysts [46]. However, in the present work, the 4*S*-diastereomer (with the *cis* arrangement of the nonyl and hydroxyl groups) predominates only over weakly acid halloysite nanotubes (Fig. 7a). The

influence of the intermediates structure in the Prins reaction on stereoselectivity will be discussed below.

According to [16], the analgesic effect was studied for a mixture of 4*S*- and 4*R*-isomers of hexahydro-2*H*-chromene-4,8-diol **2** in the ratio of 1:1, while bioactivity of individual stereoisomers or a mixture containing an excess of one of them was not carried out. Using halloysite nanotubes makes it possible to obtain mainly 4*S*-diastereomer in the reaction mixture (Table 3), which can have a significant effect on its analgesic activity.

Differences in the clays acidity are determined by peculiarity of their structure. Thus, in montmorillonites and illites, an isomorphic substitution of Al³⁺ for Si⁴⁺ in tetrahedral Si–O layers and Mg²⁺, Fe²⁺ for Al³⁺ in octahedral Al–O layers is typical [47]. For example, montmorillonite K-10 and illite contain 18.4 and 24.1% of Al³⁺ atoms in tetrahedral layers, respectively [38, 39]. As a result, a negative charge arises on the surface, which is compensated by exchangeable cations, including H₃O⁺. In illite, exchangeable ions are found mainly on the particles surface, and in montmorillonite also in the interlayer space [47], which is the reason for larger acidity of the latter.

In halloysite, 99% of Al³⁺ ions are located in octahedral layers, implying that the charges of the layers are balanced, and acid sites are located mainly at the ends and defects of nanotubes [38]. Therefore, their concentration and strength are lower than that of montmorillonite (Table S2). On this basis, the condensation of diol **1** with decanal on halloysite should occur on the outer HNT surface, while over montmorillonites the reaction happens also in the pores. Note that all studied clays are mesoporous (Table 1).

An increase in the drying temperature of halloysite immediately before the reaction led to a slight increase in the of hexahydro-2*H*-chromene-4,8-diol **2** yield and its decrease for products **3** (Table 4). However, the thermal treatment conditions have a strong influence on the stereoselectivity.

Table 4. Selectivity in the Prins reaction of diol **1*** with decanal at 40°C depending on halloysite drying temperature

HNT drying temperature, °C	r_o , mmol/L·g·min	Time, min	Selectivity, mol. %				4 <i>S</i> /4 <i>R</i>
			2	4 <i>S</i> - 2	4 <i>R</i> - 2	3	
Air-dry	5.6	180	77.3	48.1	29.2	22.7	1.6
50	14.4	120	77.8	47.5	30.3	22.2	1.6
105	29.1	90	76.9	43.9	33.0	23.1	1.3
150	47.0	30	79.8	41.7	38.1	20.2	1.1
200	20.4	60	81.2	37.8	43.4	18.8	0.9
350	12.3	120	81.5	36.4	45.1	18.5	0.8

*At 70% conversion

The largest 4*S*-isomer yield (48.1%) was observed for air-dry halloysite nanotubes. With an increase in the HNT drying temperature from 50 to 350°C, the selectivity to 4*S*-**2** decreased from 47.5 to 36.4%, at the same time increasing for to 4*R*-**2** from 30.3 to 45.1% (Table 4). Simultaneously, the 4*S*/4*R* ratio decreased from 1.6 to 0.8. Note that the initial rate of diol **1** consumption increased after halloysite drying and was the largest after its thermal treatment at 150°C (Table 4).

The change in the stereoselectivity to isomers of **2** after the halloysite thermal treatment can be explained by a change in the nature and strength of its catalytically active sites. Thus, acidity of clays is due to exchangeable and coordination-unsaturated metal ions (Lewis a.s.) as well as acidic hydroxy groups, and water molecules bound to exchange cations (Brønsted a.s.) [47, 48]. Acid-modified HNT contain both types of acid sites with a predominance of Lewis acidity (Table 2). Water molecules present on the surface of air-dry nanotubes interact with these centers according to the scheme $[L(H_2O)_x]^{z+} = [L(OH)(H_2O)_{x-1}]^{z+1} + H^+$ and act as weak Brønsted a.s. [47]. With an increase in the drying temperature of clays (i.e. surface dehydration) the concentration and strength of such a.s. increases [47, 48].

The largest yield of 4*S*-**2** was observed on air-dry halloysite nanotubes, which clearly indicates that weak Brønsted acidity favor its formation. The selectivity to 4*R*-**2** increased with an increase in the drying temperature of halloysite (Table 4) i.e. with the growth of a.s. strength and concentration. It is known that the heat treatment of clays at temperatures above 150°C leads to an increase in their Lewis acidity [49], while the highest yield of the 4*R*-**2** was observed after HNT

calcining at 350°C (Table 4). Consequently, formation of 4*R*-isomer is favored by the relatively strong Brønsted or Lewis acidity. Although the formation of both 4*R*- and 4*S*-isomers was observed at all catalyst pretreatment temperatures, the experimental results (Table 4) clearly indicate that weak Brønsted a.s. direct the reaction preferentially towards the 4*S*-2 formation.

Note that in the Prins reaction, an increase in the water content in the system leads to an increase in both overall selectivity and an increase in the yield of *cis* isomers of tetrahydropyran alcohols [38, 39, 45]. In the present work, when the drying temperature decreased (i.e. amount of water on the HNT surface increased), the ratio of stereoisomers was inverted in favor of the 4*S*- (i.e. *cis*) isomer (Table 4). A similar inversion was observed in the tandem Prins-Ritter reaction, where the addition of water before the reaction caused a sharp increase in the yield of 4*R*-amidotetrahydropyran compound [23].

An increase in the initial rate of diol **1** consumption after drying of halloysite nanotubes (Table 4) can be explained by an increase in their acidity as a result of this treatment. Note that the largest reaction rate of is observed after HNT drying at 150°C, when the concentration of Brønsted a.s. in clays is the highest [49].

Influence of acidity on the diol **1** reaction with decanal was also studied using strong Brønsted (Amberlyst-15 resin) and Lewis (scandium triflate) acids. In the presence of these catalysts, formation of predominantly dehydration products **3** was observed, while selectivity towards hexahydro-2*H*-chromene-4,8-diol **2** did not exceed 36.7% (Table 5). Note that selectivity to products **2** and **3** on Amberlyst-15 was practically independent of the diol **1** conversion (Fig. S3), which indicates their parallel formation.

Table 5. Selectivity in the Prins reaction of diol **1*** with decanal at 40°C on catalysts with different types of acidity

Catalyst**	r_0 , mmol/L·g·min	Time, min	Selectivity, mol. %				4 <i>S</i> /4 <i>R</i>
			2	4 <i>S</i> -2	4 <i>R</i> -2	3	
Amberlyst-15	179.0	5	9.8	4.6	5.2	68.6	0,9
Scandium triflate***	-	240	36.7	25.6	11.1	60.3	2.3
Halloysite	29.1	90	76.9	43.9	33.0	23.1	1.3

* At 70% conversion; ** Dried at 105°C; ***100% conversion at 20°C in CH₂Cl₂

On the other hand, a relatively high selectivity to hexahydro-2*H*-chromene-4,8-diol (76.9%) was observed in the presence of halloysite nanotubes (Table 5) with relatively weak a.s. of both types (Table 2). It should be noted that in Prins cyclization of 3-methylbutenol with aldehydes in the presence of a mixture of weak Lewis and Brønsted acids led to the selective formation of *cis*-isomers of tetrahydropyran compounds [50]. Analysis of this synergy by the DFT method showed that the coordination of Lewis acids to Brønsted (carboxylic and sulfonic) acids result in an increase in the acidity of the latter [50]. Similarly, the interaction of water molecules with Lewis a.s. in halloysite results in appearance of weak Brønsted a.s. properties in H₂O [47] and the predominant formation of the 4*S*-isomer.

Worth noting that in the presence of a H(Fe)-Beta zeolite and Ce-MCM-41 mesoporous material, exhibiting both types of acidity, diol **1** condensation with benzaldehyde gave the corresponding hexahydro-2*H*-chromene-4,8-diol with approximately the same (64–67%) selectivity [15]. However, the effect of catalysts on stereoselectivity of the reaction in that work was not reported.

3.2. Influence of the reaction temperature and catalysts concentration

Condensation of diol **1** with decanal at 20°C practically did not occur, whereas at 30°C for 6 h, the conversion of **1** was only 19%. Elevation of the reaction temperature from 40 to 60°C gave an increase in the initial consumption rate of **1**, while a slight decrease in the overall selectivity to hexahydro-2*H*-chromene-4,8-diol **2** and a slight increase in the selectivity for products **3** were observed (Table 6)

Table 6. Selectivity in the Prins reaction of diol **1*** with decanal over halloysite** at different temperatures

Reaction temperature	r _o , mmol/L·g·min	Time, min	Selectivity, mol. %				4 <i>S</i> /4 <i>R</i>
			2	4 <i>S</i> - 2	4 <i>R</i> - 2	3	
40	5.6	180	77.3	48.1	29.2	22.7	1.6
50	15.0	60	76.5	49.0	27.5	23.5	1.8
60	41.0	20	75.0	49.4	25.6	25.0	1.9

*At 70% conversion; **In air-dry state

At 40°C selectivity to diastereomers of hexahydro-2*H*-chromene-4,8-diol **2** and to products **3** initially did not depend on the diol **1** conversion (Fig. 8), pointing out on the parallel formation of these compounds. A slight decrease in selectivity to 4*S*-**2** and its increase to 4*R*-**2** as a function of diol conversion at 40°C (Fig. 8a) can be explained by the isomerization of 4*S*- to 4*R*-isomer.

At a larger reaction temperature (50 and 60°C), with an increase in diol **1** conversion, the selectivity to 4*S*-**2** decreased in a more prominent way, while to 4*R*-**2** practically did not change (Fig. 8a). At the same time, a substantial increase of products **3** yield and a decrease in the 4*S*/4*R* isomers ratio were observed (Fig. 8b,c). Thus, Fig. 8a,b indicates that 4*S*-isomer undergoes dehydration into compounds **3**.

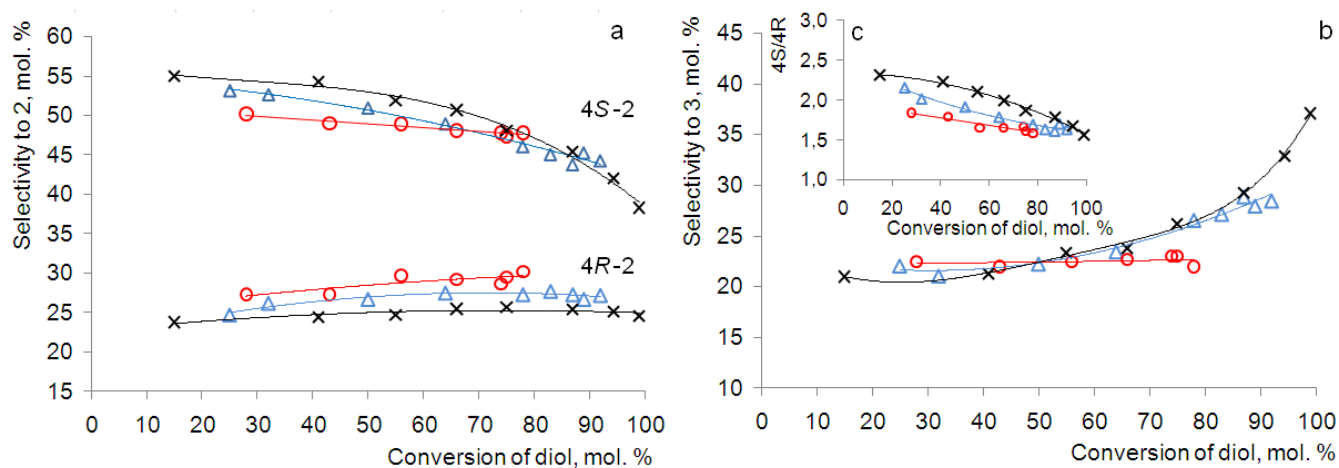


Fig. 8. Selectivity to hexahydro-2*H*-chromene-4,8-diol isomers (a), dehydration products (b) and isomers ratio (c) as a function of diol conversion on halloysite at 40 (○), 50 (Δ) and 60°C (X)

Note that in a similar reaction of (-)-isopulegol with thiophene-2-carbaldehyde, partial dehydration of the 4*R*-isomer (with *cis* arrangement of substituents) was reported, which, according to [38], may be because of its preferable adsorption on the catalyst surface. On the other hand, in the Prins reaction of (-)-isopulegol with acetone, selectivity to 4*R*- and 4*S*-isomers increased with an increase in conversion due to backward reaction of the ester of isopulegol with chromenol [21, 39].

In the diol **1** Prins condensation with decanal on air-dry HNT, an increase in the catalyst to reagent ratio gave a slight increase in the overall selectivity to the 4*S*-isomer of hexahydro-2*H*-chromene-4,8-diol **2**, while selectivity to the 4*R*-isomer remained practically constant (Table 7). In the case of diol **1** condensation with decanal on halloysite dried at 350°C, a slight decrease in the yield of both compound **2** and its 4*S*-diastereomer was observed (Table 7).

According to [38], in the case of (-)-isopulegol condensation with thiophene-2-carbaldehyde, an increase in the concentration of air-dry halloysite led to an increase in the yield of the 4*R*-isomer of octahydro-2*H*-chromen-4-ol. Kinetic modeling showed the second order in the catalyst, which indicates participation of water on the catalyst surface in the reaction. The mechanism proposed in [38] for this isomer production includes formation of cyclic intermediate at weak acid sites followed by the transfer of H₂O from the catalyst surface to this intermediate (Fig. S4). Based on this, it can be assumed that formation of 4*S*-isomer of hexahydro-2*H*-chromene-4,8-diol **2** is facilitated by the presence of adsorbed water in halloysite, which can participate in the reaction.

Table 7. Selectivity in the Prins reaction of diol **1*** with decanal at 40°C over halloysite

Catalyst/reagent ratio (g/g)	Time, min	Selectivity, mol. %				4 <i>S</i> /4 <i>R</i>
		2	4 <i>S</i> - 2	4 <i>R</i> - 2	3	
Air-dry						
0.5	360	74.2	44.8	29.4	25.8	1.5
1.0	120	78.2	48.1	30.1	21.8	1.6
2.0	140	77.8	49.4	28.4	22.2	1.7
Dried at 350°C						
0.5	120	79.1	32.8	46.3	17.0	0.7
1.0	30	78.2	30.3	47.9	17.1	0.6
2.0	10	76.2	29.7	46.5	16.7	0.6

*At 60% conversion

3.3. Mechanistic discussion

In accordance with the generally accepted mechanism for the Prins cyclization [50], the reaction of diol **1** with decanal leads to formation of a cyclic tertiary carbocation **2-A**, subsequent addition of water to which gives hexahydro-2*H*-chromene-4,8-diol **2** as 4*S*- and 4*R*-diastereomers (Fig. 9). This reaction route dominates in the presence of clays with a relatively low acidity

(halloysite, illite, and montmorillonite), resulting in formation of isomers of **2** in a parallel mode. Only 4*S*-isomer can undergo dehydration with the products **3** formation (Fig. 8), which may be explained by its preferable adsorption on the catalyst surface.

In the presence of strong Brønsted (Amberlyst-15) and Lewis (scandium triflate) acids, the main products were chromenes **3**, mainly formed directly from the reagents, which follows from the selectivity curves for products **2** and **3** formation (Fig. S3).

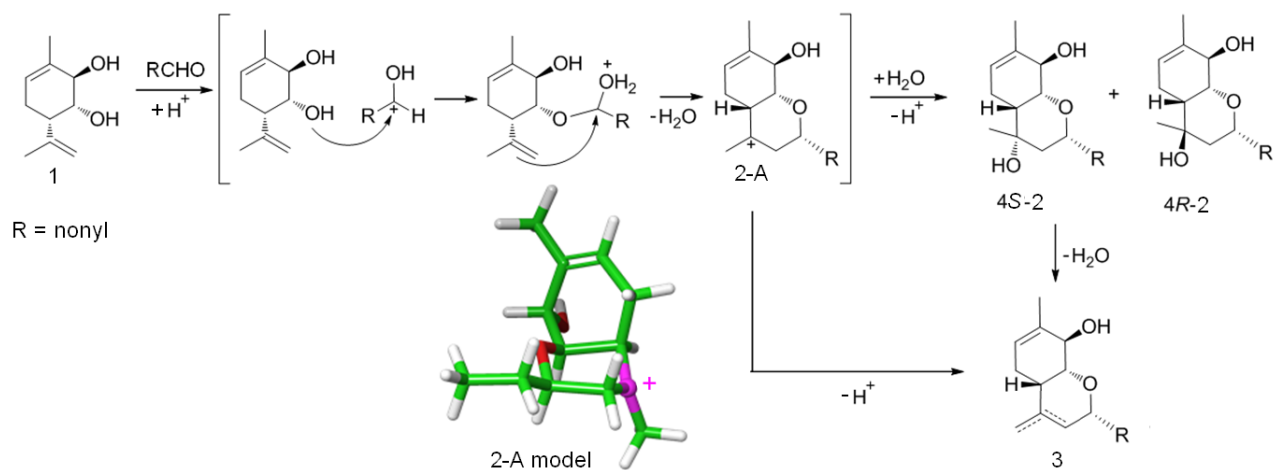


Fig. 9. The mechanism of diol condensation with decanal and the DFT optimized structure of the key intermediate

For further evaluation of the reasons of 4*S*-**2** predominance in the reaction products over halloysite, DFT geometry optimization was performed for the tertiary carbocation **2-A**, which is the key intermediate in the hexahydro-2*H*-chromene-4,8-diol **2** formation.

Initially, DFT calculations at B3LYP/6-31G** level for 4-methyltetrahydropyranyl cation in the chair form (Fig. S5) were performed. In this ion, the CH₂–CH₂ bonds are exceptionally long, while the C–C bonds to the carbocation center and the C–O bonds are shortened. In the cation the C⁺–CH₃ is semi-axial to provide a better overlap of the empty *p*-orbital with the CH₂–CH₂ bond orbitals [51] and the equatorial lone pair on oxygen, forming a 6-electron system in the equatorial plane of the 6-member ring [52].

Further, geometry optimization was performed at the same DFT level for model **2-A** carbocations with the ethyl group instead of a long chain nonyl group. Such simplification does not affect significant geometry of the chromene scaffold, simultaneously decreasing the computation time. Conformation of the tetrahydropyran moiety in the **2-A** model cation (Fig. 9) matches the structure of the 4-methyltetrahydropyranyl ion (Fig. S5) and C⁺-CH₃ moiety is semi-axial. Based on this, the nucleophile capture more preferably is taking place via the equatorial approach forming 4*S*-isomer of hexahydro-2*H*-chromene-4,8-diol. Thus, the DFT study of a key intermediate **2-A** in Prins cyclization predicted 4*S*-diastereomer formation of product **2** based on the most stable geometry of this intermediate.

Thus, it can be assumed that in the presence of weakly acidic (45 μmol/g) halloysite nanotubes, intermediate **2-A** is adsorbed on the surface predominantly in the conformation that favors the nucleophile (H₂O) attack at the equatorial position with formation of the 4*S*-isomer (Fig. 9). Presence of absorbed water molecules on the halloysite surface should favor their transfer from the surface to the **2-A** and increase the selectivity to 4*S-2*, which was observed on air-dry HNT (Table 4).

Over montmorillonites K-10 and K-30 with a relatively high acidity (up to 104 μmol/g), the Prins condensation of diol **1** with decanal leads mainly to of 4*R-2* in the reaction products (Fig. 5a). In this case, the conformation of **2-A** ion, which is adsorbed on the stronger a.s. should be different and favoring formation of the 4*R*-isomer of hexahydro-2*H*-chromene-4,8-diol **2**.

For quantitative description of the reaction kinetics a simplified reaction network **based on the experimental results** was used (Fig. 10). Details of kinetic modelling are presented in Supporting Information.

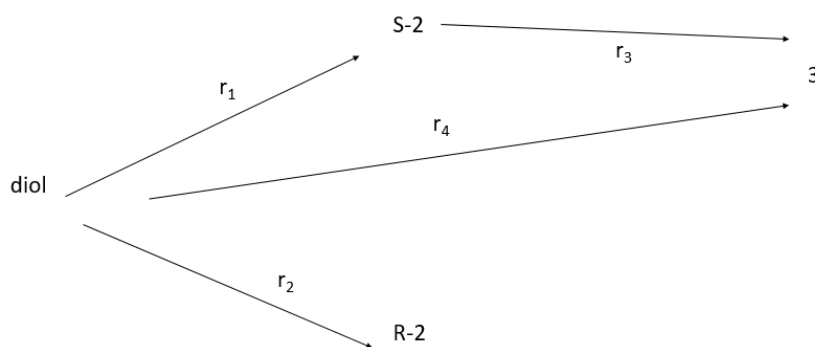


Fig. 10. Simplified reaction network for synthesis of hexahydro-2*H*-chromenes.

A pseudo first order model was used by incorporating the aldehyde concentration in the rate constant. The initial modelling included in the rate equations adsorption coefficients of all reactants, however, while during parameter estimation it turned out that inclusion of only the adsorption coefficient of component **3** is sufficient to describe the experimental data. This result points out on a stronger adsorption of this compound most probably due to presence of the olefinic bond outside of the ring.

The degree of explanation, reflecting comparison between the residuals given by the model to the residuals of the simplest model, i.e. the average value of all the data points, was 98%, confirming that the experimental data could be described in an adequate way by the proposed reaction network (Fig. S6). The values of activation energies for formation of both isomers of compound 2 are almost the same (i.e. 103 and 106 kJ/mole for 4*S*-2 and 4*R*-2, respectively), which can point out on the common rate limiting step prior to differentiating between the isomers of compound 2. In the case of (-)-isopulegol reaction with thiophene-2-carbaldehyde on HNT, the activation energies also practically did not differ, being although significantly lower (55–58 kJ/mol) [38]. The errors of the parameters (Table S1) are also rather low apart from the dehydration step of 4*S*-2 to compound **3**.

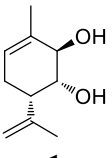
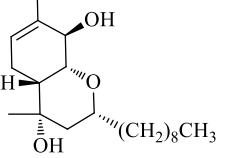
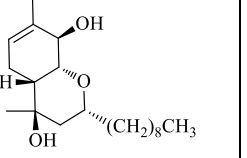
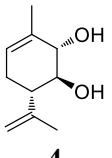
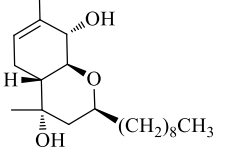
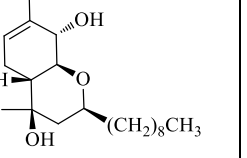
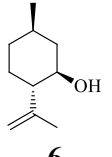
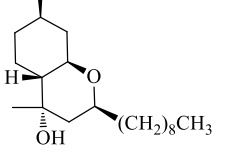
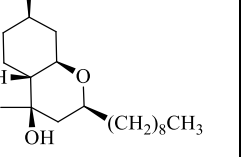
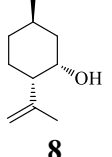
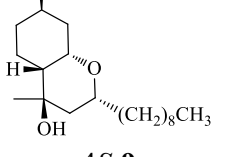
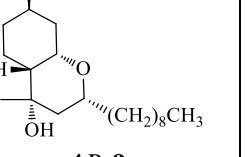
Based on the kinetic data generated in the current work it is difficult to conclude which pathway of the compound **3** formation is preferential (i.e. r_3 or r_4 in Fig. 10) due to an apparent compensation effect between the pre-exponential factors and the activation energies of these steps.

On the other hand, according to experimental data (Fig. 8), the dehydration of the 4*S*-isomer clearly proceeded only at 60°C

3.4. Reaction scope and catalyst stability

Condensation of a number of terpene alcohols (isomeric diols **1** and **4**, isopulegol **6**, neoisopulegol **8**) with decanal on halloysite nanotubes led to formation of the corresponding chromenols as 4*S*- and 4*R*-diastereomers (Table 8). Thus, in the case of diols **1** and **4**, 4*S*-isomers were mainly observed, while isopulegol **6** gave primarily the 4*R*-stereoisomer. Condensation of neoisopulegol **8** with decanal resulted in equal amounts of the isomers (Table 8).

Table 8. Products of the terpene alcohols reaction with decanal over halloysite* at 40°C in toluene

Terpene alcohol	Resulting compounds		Yield, %	4 <i>S</i> /4 <i>R</i>
 1	 4<i>S</i>-2	 4<i>R</i>-2	77,3**	1.6:1
 4	 4<i>S</i>-5	 4<i>R</i>-5	36	1.3:1
 6	 4<i>S</i>-7	 4<i>R</i>-7	75	1:2.7
 8	 4<i>S</i>-9	 4<i>R</i>-9	68	1:1

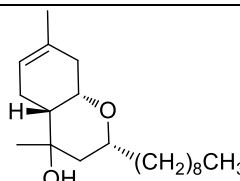
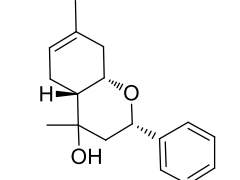
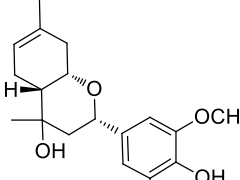
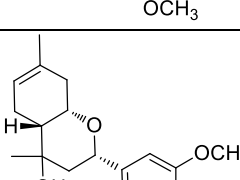
*In air-dry state; **GC yield

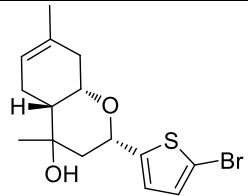
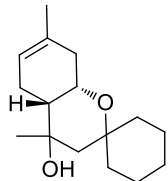
According to DFT (B3LYP/6-31G**) optimization of the model intermediates **2-A**, **5-A**, **7-A**, and **9-A** (Fig. S7), in all cases the geometry of these species favors the attack of the nucleophile to

the equatorial position. The products corresponding to this addition are formed as the main ones in the case of diol **1** (4*S*-**2**) and isopulegol **6** (4*R*-**7**). In the reaction of decanal with neoisopulegol **8** and diol **4**, the 4*S*/4*R* isomers ratio was close to unity, or slightly above it (Table 8), which may indicate a change in the conformation of intermediates as a result of adsorption on the halloysite surface.

An overview the results for diol **1** condensation with various carbonyl compounds in the presence of halloysite in an air-dry state, as well as a comparison with previous results on other catalysts, is given in Table 9. The reaction was carried out at room temperature without a solvent, because under these conditions, synthesis of hexahydro-2*H*-chromene-4,8-diols is usually carried out [16]. The reactions proceed with from moderate to high yields with predominant formation of 4*S* isomers and 4*S*/4*R* ratio up to 21 (Table 9).

Table 9. Products yields and stereoisomers ratio in the diol **1** reaction with carbonyl compounds*

Entry	Carbonyl compound	Catalyst	Resulting hexahydro-2 <i>H</i> -chromene-4,8-diol 2	Yield, %	4 <i>S</i> /4 <i>R</i>	Ref.
1	Decanal	HNT		79	1.9	This work
		K-10		60	1.0	16
2	Benzaldehyde	HNT		88**	4.2	This work
		K-10		43	1.0	13
		H-Beta-25		67***	n.d.	15
		H-Beta-300		64***	--/--	--/--
		Ce-MCM-41		67***	--/--	--/--
3	4-Hydroxy-3,5-dimethoxybenzaldehyde (syringaldehyde)	HNT		58	7.3	This work
		K-10		26	2.0	13
4	2,4,5-Trimethoxybenzaldehyde	HNT		53	3.6	This work
		K-10		39	2.1	14

5	5-Bromothiophene-2-carbaldehyde	HNT		56	1.5	This work
		K-10		47	1.3	13
6	Cyclohexanone	HNT		67**	21.0	This work
		K-10		51	2.0	53

*Solvent free, for 24 h at room temperature; **GC yield; ***In toluene at 70°C, GC data

In all cases, the use of halloysite nanotubes led to an increase in the total yield of the corresponding hexahydro-2*H*-chromene-4,8-diols **2** and higher 4*S*/4*R* isomers ratio in comparison with K10 clay. Thus, in the presence of K-10 clay, the Prins condensation of diol **1** with benzaldehyde and its derivatives gave rather low (up to 43%) yields of **2**, which increased up to 88% on halloysite (Table 9, entry 2), along with increase of the 4*S*/4*R* ratio up to 7.3 (Table 9, entry 3). The reaction of diol **1** with substituted aromatic aldehydes on HNT (Table 9, entry 3–5) exhibited lower selectivity than in the case of benzaldehyde (Table 9, entry 2). Note that many products of the reaction of terpenoid **1** with benzaldehydes containing hydroxy- and methoxy- groups show pronounced analgesic and antiviral activity [13].

Condensation of diol **1** with cyclohexanone in the presence of halloysite led to the impressive stereoselective formation of the spirocyclic product (Table 9, entry 6) with a very high ratio of 4*S*/4*R* diastereomers (21.0), while at K-10 it was only 2.0 (Table 9, entry 6). The yield of the corresponding hexahydro-2*H*-chromene-4,8-diol also increased from 51 to 67%. It is important to note that this compound has a high analgesic activity, which is significantly higher than that for diclofenac sodium [53].

An increase in selectivity to the 4*S*-isomers on halloysite in the case of all studied carbonyl compounds is consistent with the DPT calculations, according to which addition of the nucleophile (H₂O) occurs at the equatorial position.

In general, the obtained results show that the use of acid-modified halloysite nanotubes made possible a significant increase of the total yield of chromene alcohols and the ratio of diastereomers. The practical significance of halloysite nanocatalysts lies in the possibility of obtaining individual stereoisomers and studying their biological activity.

To study the catalyst stability, after the reaction of diol **1** with decanal at 40°C over halloysite, the latter was separated from the reaction mixture, washed three times with ethyl acetate, then distilled water, dried at 105°C, and kept in air for 12 h before reuse.

The diol **1** conversion after 6 h of reaction was 77.8% in the presence of the fresh catalyst and decreased to 66.3% after the third cycle (Table 10). In this case, the overall selectivity towards hexahydro-2*H*-chromene-4,8-diol **2** and the stereoisomers ratio remained practically unchanged .

Table 10. Selectivity in the Prins condensation of diol **1** with decanal over halloysite* for 6 h at 40°C depending on halloysite utilization cycles

Halloysite utilization cycle	Diol conversion, %	Selectivity, mol. %				4 <i>S</i> /4 <i>R</i>
		2	4 <i>S</i> - 2	4 <i>R</i> - 2	3	
1 (fresh)	77.8	78.0	47.8	30.2	22.0	1.6
2	70.1	79.4	48.1	31.3	20.6	1.5
3	66.3	78.6	47.0	31.6	21.4	1.5

*In air-dry state

Thus, the catalytic properties of halloysite were retained over three reaction cycles, although there was a slight loss of activity. It is important to note that, according to [34, 36], the reuse of HNT in the condensation of isopulegol or 2-carene with aldehydes did not lead to a substantial decrease in its acidity and specific surface area, and the shape and size of nanotubes were completely preserved.

Overall, this work is the first systematic study of the *p*-menta-1,8-diene-5,6-diol catalytic condensation with aldehydes. In contrast to the well-studied Prins reaction of (-)-isopulegol with carbonyl compounds, where in all cases the 4*R*-isomer was the main one [19, 38, 39], the diol condensation led to formation of practically equal amounts of stereoisomers [16]. Nevertheless, the use of halloysite nanotubes can significantly increase the stereoselectivity of this reaction towards the 4*S*-isomers. Utilization of diol and (-)-isopulegol as well as optimization of the key intermediates

geometry for these molecules allowed for the first time to conclude that, in the presence of halloysite nanocatalysts, the attack of the nucleophile (H₂O) occurs in the equatorial position, which is fully consistent with the experimental results.

Conclusions

The condensation of α -pinene derived *p*-menta-1,8-diene-5,6-diol (diol) with decanal was studied for the first time in the presence of acid-modified halloysite nanotubes (HNT), as well as illite and commercial montmorillonites K-10 and K-30. The choice of the reagents was due to the high analgesic activity of the resulting hexahydro-2*H*-chromene-4,8-diol (as 4*S*- and 4*R*-diastereomers). The catalysts were previously thoroughly characterized by a range advanced physico-chemical methods. The catalytic properties of halloysite have also been studied in decanal reactions with a number of terpene alcohols as well as in diol condensation with a set of carbonyl compounds.

In the case of diol condensation with decanal, the total yield of hexahydro-2*H*-chromene-4,8-diol in toluene at 40°C was almost independent on the used aluminosilicate catalyst being 76–80%. However, the selectivity towards 4*S*-isomer decreased from 48.1 to 34.6%, increasing to 4*S*-isomer from 29.2 to 43.6% with an increase in the catalyst acidity from 45 to 104% $\mu\text{mol/g}$, respectively. Formation of 4*S*-diastereomer was favored by the weak acidity of halloysite. On the other hand, in the presence of strong Brønsted (Amberlyst-15) and Lewis (scandium triflate) acids the total yield of these isomers was no more than 37% because of dehydration products formation. An increase in the HNT drying temperature from 50 to 350°C leads to a decrease in the 4*S*/4*R* isomers ratio of hexahydro-2*H*-chromene-4,8-diol from 1.6 to 0.8, respectively. A decrease in the selectivity to 4*S*-diastereomer from 48.1% for air dry halloysite to 36.4% for one dried at 350°C clearly indicates the key role of weak Brønsted acidity in its formation.

The mechanism and ways of the formation products of diol condensation with decanal were discussed. Optimization of the key carbocation geometry using the density functional theory showed

that the attack of the nucleophile should preferably take place in the equatorial position, i.e. with the formation of the 4*S*-isomer, which was observed for weakly acidic halloysite nanotubes.

In the case of diol condensation with carbonyl compounds at room temperature without a solvent on halloysite, the yield of hexahydro-2*H*-chromene-4,8-diols (up to 88.0%) and the 4*S*/4*R* isomers ratio (up to 21.0) were significantly higher than on other catalysts, which can simplify the isolation of individual stereoisomers for the study of their biological activity. Stability of the catalytic properties of HNT was also shown.

Overall, halloysite nanotubes should be considered as selective and stable catalysts for the preparation of terpenoid-based heterocyclic compounds.

Acknowledgments

The research was financially supported by Belarusian Republican Foundation for Fundamental Research (BRFFR, grant X19RM-002) and Russian Foundation for Basic Research (RFBR, grant 19-53-04005 Bel_mol_a).

Conflict of interest

The authors declare that there is no conflict of interest

References

1. A.L. Harvey, R.A. Edrada-Ebel, R.J. Quinn. The re-emergence of natural products for drug discovery in the genomics era. *Nat. Rev. Drug Discov.*, 2015, 14, 111–129.
2. D.J Jansen, R.A Shenvi, Synthesis of medicinally relevant terpenes: reducing the cost and time of drug discovery, *Future Med. Chem.*, 2014, 6, 1127–1148.
3. R. Jaeger, E. Cuny, Terpenoids with special pharmacological significance: A review, *Nat. Prod. Commun.*, 2016, 11, 1373 – 1390.
4. D.N. Gouveia, A.G. Guimarães, W.B. da Rocha Santos, L.J. Quintans-Júnior, Natural products as a perspective for cancer pain management: a systematic review, *Phytomedicine*, 2019, 58, 152766.
5. I.V. Il'ina, N.S. Dyrkheeva, A.L. Zakharenko, A.Y. Sidorenko, N.S. Li-Zhulanov, D.V. Korchagina, R. Chand, D.M Ayine-Tora, A.A. Chepanova, O.D. Zakharova, E.S. Ilina, J. Reynisson, A.A. Malakhova, S.P. Medvedev, S.M. Zakian, K.P. Volcho, N.F. Salakhutdinov, O.I Lavrik, Design, synthesis, and biological investigation of novel classes of 3-carene-derived potent inhibitors of TDP1, *Molecules*, 2020, 25, 3496.
6. M. Zielińska-Błajet, J. Feder-Kubis, Monoterpenes and their derivatives – recent development in biological and medical applications, *Int. J. Mol. Sci.*, 2020, 21, 7078.
7. Terpenoids Against Human Diseases, ed. D.N. Roy, CRC Press, Boca Raton, 2019.
8. L. Jørgensen, S.J. McKerrall, C.A. Kuttruff, F. Ungeheuer, J.Felding, P.S. Baran, 14-Step synthesis of (+)-ingenol from (+)-3-carene, *Science*, 2013, 341, 878–882.
9. A.J.D. Silvestre, A. Gandini, Chapter 2. Terpenes: Major Sources, Properties and Applications in Monomers, Polymers and Composites from Renewable Resources, ed. M. N. Belgacem and A. Gandini, *Elsevier*, Amsterdam, 2008, 17–38.
10. I.V. Il'ina, K.P. Volcho, D.V. Korchagina, V.A. Barkhash, N.F. Salakhutdinov, Reactions of allyl alcohols of the pinane series and of their epoxides in the presence of montmorillonite clay, *Helv. Chim. Acta*, 2007, 90, 353–368.

11. O.V. Ardashov, A.V. Pavlova., I.V. Il'ina, E.A. Morozova, D.V. Korchagina, E.V. Karpova, K.P. Volcho, T.G. Tolstikova, N.F. Salakhutdinov, Highly potent activity of (1R,2R,6S)-3-methyl-6-(prop-1-en-2-yl)cyclohex-3-ene-1,2-diol in animal models of Parkinson's disease. *J. Med. Chem.*, 2011, 54, 3866–3874.
12. E. Valdman, I. Kapitsa, E. Ivanova, T. Voronina, O. Ardashov, K. Volcho, V. Khazanov, N. Salakhutdinov, Evolution of anti-parkinsonian activity of monoterpenoid (1R,2R,6S)-3-methyl-6-(prop-1-en-2-yl)cyclohex-3-ene-1,2-diol in various in vivo models, *Eur. J. Pharmacol.*, 2017, 815, 351–363.
13. O.S. Patrusheva, K.P. Volcho, N.F. Salakhutdinov, Synthesis of oxygen-containing heterocyclic compounds based on monoterpenoids, *Russ. Chem. Rev.*, 2018, 87, 771–796
14. O. Mikhailchenko, I. Il'ina, A. Pavlova, E. Morozova, D. Korchagina, T. Tolstikova, E. Pokushalov, K. Volcho, N.Salakhutdinov, Synthesis and analgesic activity of new heterocyclic compounds derived from monoterpenoids, *Med. Chem. Res.*, 2013, 22, 3026–3034.
15. M. Stekrova, P. Mäki-Arvela, N. Kumar, E. Behraves, A. Aho, Q. Balme, K.P. Volcho, N.F. Salakhutdinov, D.Yu. Murzin, Prins cyclization: Synthesis of compounds with tetrahydropyran moiety over heterogeneous catalysts, *J. Mol. Catal. A: Chem.*, 2015, 410, 260–270.
16. I. Il'ina, A. Pavlova, D. Korchagina, O. Ardashov, T. Tolstikova, K. Volcho, N. Salakhutdinov, Synthesis and analgesic activity of monoterpenoid-derived alkyl-substituted chiral hexahydro-2H-chromenes, *Med. Chem. Res.*, 2017, 26, 1415–1426.
17. I.V. Ilyina, V.V. Zarubaev, I.N. Lavrentieva, A.A. Shtro, I.L. Esaulkova, D.V. Korchagina, S.S. Borisevich, K.P. Volcho, N.F. Salakhutdinov, Highly potent activity of isopulegol-derived substituted octahydro-2H-chromen-4-ols against influenza A and B viruses. *Bioorg. Med.Chem. Lett.*, 2018, 28, 2061–2067.
18. A. Pavlova, O. Mikhailchenko, A. Rogachev, I. Il'ina, D. Korchagina, Y. Gatilov, T. Tolstikova, K. Volcho, N. Salakhutdinov, Synthesis and analgesic activity of stereoisomers of 2-(3(4)-hydroxy-4(3)-methoxyphenyl)-4,7-dimethyl-3,4,4a,5,8,8a-hexahydro-2H-chromene-4,8-diols. *Med. Chem. Res.*, 2015, 24, 3821–3830.

19. G. Baishya, B. Sarmah, N. Hazarika, An environmentally benign synthesis of octahydro-2*H*-chromen-4-ols via modified montmorillonite K10 catalyzed Prins reaction, *Synlett*, 2013, 24, 1137–1141.
20. M.N. Timofeeva, V.N. Panchenko, A. Gil, S.V. Zakusin, V.V. Krupskaya, K.P. Volcho, M.A. Vicente, Effect of structure and acidity of acid modified clay materials on synthesis of octahydro-2*H*-chromen-4-ol from vanillin and isopulegol, *Catal. Commun.*, 2015, 69, 234–238.
21. M. Laluc, P. Maki-Arvela, A.F. Peixoto, N. Li-Zhulanov, T. Sandberg, N.F. Salakhutdinov, K. Volcho, C. Freire, A.Yu. Sidorenko, D.Yu. Murzin. Catalytic synthesis of bioactive 2*H*-chromene alcohols from (-)-isopulegol and acetone on sulfonated clays. *Reac. Kinet. Mech. Cat.*, 2020, 129, 627–644.
22. A.O. Zaykovskaya, N. Kumar, E.A. Kholkina, N.S. Li-Zhulanov, P. Maki-Arvela, A. Aho, J. Peltonen, M. Peurla, I. Heinmaa, B.T. Kusema, S. Streiff, D.Yu. Murzin, Synthesis and physico-chemical characterization of Beta zeolite catalysts: Evaluation of catalytic properties in Prins cyclization of (-)-isopulegol, *Micropor. Mesopor. Mat.*, 2020, 302, 110236.
23. A.Yu. Sidorenko, N.S. Li-Zhulanov, P. Mäki-Arvela, T. Sandberg, A.V. Kravtsova, A.F. Peixoto, C. Freire, K.P. Volcho, N.F. Salakhutdinov, V.E. Agabekov, D.Yu. Murzin, Stereoselectivity inversion by water addition in the tandem Prins-Ritter reaction for synthesis of 4-amidotetrahydropyran derivatives, *ChemCatChem*, 2020, 12, 2605 – 2609.
24. L.F. Silva Jr., S.A. Quintiliano, An expeditious synthesis of hexahydrobenzo[*f*]isochromenes and of hexahydrobenzo[*f*]isoquinoline via iodine-catalyzed Prins and aza-Prins cyclization, *Tetrahedron Lett.* 50 (2009) 2256–2260.
25. J.S. Yadav, B.V. Subba Reddy, A.V. Ganesh, G.G.K.S. Narayana Kumar, Sc(OTf)₃-catalyzed one-pot ene-Prins cyclization: a novel synthesis of octahydro-2*H*-chromen-4-ols, *Tetrahedron Lett.* 2020, 51, 2963–2966.

26. B. Sarmah, G. Baishya, R.K. Baruah, First example of a Prins –Ritter reaction on terpenoids: a diastereoselective route to novel 4-amido-octahydro-2*H*-chromenes, *RSC Adv.*, 2014, 4, 22387–22397.
27. S. Slater, P.B. Lasonkar, S. Haider, M.J. Alqahtani, A.G. Chittiboyina, I.A. Khan, One-step, stereoselective synthesis of octahydrochromanes via the Prins reaction and their cannabinoid activities, *Tetrahedron Lett.* 2018, 59, 807–810.
28. M. Massaro, R. Noto, S. Riela, Past, present and future perspectives on halloysite clay minerals, *Molecules*, 2020, 25, 4863.
29. P. Yuan, D Tan, F. Annabi-Bergaya, Properties and applications of halloysite nanotubes: recent research advances and future prospects, *Appl. Clay. Sci.*, 2015, 112–113, 75–93.
30. N. Danyliuk, J. Tomaszewska, T. Tatarchuk, Halloysite nanotubes and halloysite-based composites for environmental and biomedical applications, *J. Mol. Liq.*, 2020, 309, 113077.
31. X. Zhao, C. Zhou, M. Liu, Self-assembled structures of halloysite nanotubes: towards the development of high-performance biomedical materials. *J. Mat. Chem. B*, 2020, 8, 838–851.
32. S. Sadjadi, Halloysite-based hybrids/composites in catalysis, *Appl. Clay Sci.*, 2020, 189, 105537.
33. A. Mahajan, P. Gupta, Halloysite nanotubes based heterogeneous solid acid catalysts, *New J. Chem.*, 2020, 44, 12897–12908.
34. M. Massaro, C.G. Colletti, G. Buscemi, S. Cataldo, S. Guernelli, G. Lazzara, L.F. Liotta, F. Parisi, A. Pettignano, S. Riela, Palladium nanoparticles immobilized on halloysite nanotubes covered by a multilayer network for catalytic applications, *New J. Chem.*, 2018, 42, 13938–13947.
35. J. Hamdi, A. A. Blanco, B. Diehl, J. B. Wiley, M. L. Trudell, Room-temperature aqueous Suzuki–Miyaura cross-coupling reactions catalyzed via a recyclable palladium@halloysite nanocomposite, *Org. Lett.*, 2019, 21, 10, 3471–3475
36. A. Stavitskaya, K. Mazurova, M. Kotelev, O. Eliseev, P. Gushchin, A. Glotov, R. Kazantsev, V. Vinokurov, Yu. Lvov, Ruthenium-loaded halloysite nanotubes as mesocatalysts for Fischer–Tropsch synthesis, *Molecules*, 2020, 25, 1764.

37. Y. Zhang, B. Li, W. Guan, Y. Wei, C. Yan, M. Meng, J. Pan, Y. Yan, One-pot synthesis of HMF from carbohydrates over acid-base bi-functional carbonaceous catalyst supported on halloysite nanotubes, *Cellulose*, 2020, 27, 3037–3054.
38. A.Yu. Sidorenko, A.V. Kravtsova, A. Aho, I. Heinmaa, H. Pazniak, K.P. Volcho, N.F. Salakhutdinov, D.Yu. Murzin, V.E. Agabekov, Highly selective Prins reaction over acid-modified halloysite nanotubes for synthesis of isopulegol-derived 2H-chromene compounds, *J. Catal.*, 2019, 374, 360 – 377.
39. A.Yu. Sidorenko, A.V. Kravtsova, I.V. Il'ina, J. Wärnå, D.V. Korchagina, Yu.V. Gatilov, K.P. Volcho, N.F. Salakhutdinov, D.Yu. Murzin, V.E. Agabekov. Clay nanotubes catalyzed solvent-free synthesis of octahydro-2H-chromenols with pharmaceutical potential from (-)-isopulegol and ketones, *J. Catal.*, 2019, 380, 145 – 152.
40. A.Yu. Sidorenko, A.V. Kravtsova, P. Mäki-Arvela, A. Aho, T. Sandberg, I.V. Il'ina, N.S. Li-Zhulanov, D.V. Korchagina, K.P. Volcho, N.F. Salakhutdinov, D.Yu. Murzin, V.E. Agabekov. Synthesis of isobenzofuran derivatives from renewable 2-carene over halloysite nanotubes, *Mol. Catal.*, 2020, 490, 110974.
41. O.S. Mikhalchenko, D.V. Korchagina, K.P. Volcho, N.F. Salakhutdinov. Formation of the Compounds with an Epoxychromene Framework: Role of the Methoxy Groups. *Helv. Chim. Acta*, 2014, 97, 1406–1421.
42. E. Nazimova, A. Pavlova, O. Mikhalchenko, I. Il'ina, D. Korchagina, T. Tolstikova, K. Volcho, N. Salakhutdinov, Discovery of highly potent analgesic activity of isopulegol-derived (2R,4aR,7R,8aR)-4,7-dimethyl-2-(thiophen-2-yl)-octahydro-2H-chromen-4-ol, *Med. Chem. Res.*, 2016, 25, 1369–1383.
43. A.Yu. Sidorenko, A.V. Kravtsova, A. Aho, I. Heinmaa, T.F. Kuznetsova, D.Yu. Murzin, V.E. Agabekov, Catalytic isomerization of α -pinene oxide in the presence of acid-modified clays. *Mol. Catal.*, 2018, 448, 18–29.
44. Jaguar, Schrödinger, LLC, New York, NY, 2018.

45. L. Sekerová, E. Vyskočilová, L. Červený, Prins cyclization of isoprenol with various aldehydes using MoO₃/SiO₂ as a catalyst, *Reac. Kinet. Mech. Cat.*, 2017, 121, 83–95.
46. A.Yu. Sidorenko, Yu.M. Kurban, A. Aho, Zh.V. Ihnatovich, T.F. Kuznetsova, I. Heinmaa, D.Yu. Murzin, V.E. Agabekov, Solvent-free synthesis of tetrahydropyran alcohols over acid-modified clays, *Mol. Catal.*, 2021, 499, 111306.
47. F. Bergaya, G. Lagaly, Handbook of clay science, Part A: Fundamental, 2013, Elsevier, Amsterdam.
48. S. Yariv, H. Cross, Organo-Clay Complexes and Interactions. Marcel Dekker, New York, 2002.
49. D.R. Brown, C.N. Rhodes, Brønsted and Lewis acid catalysis with ion-exchanged clays, *Catal. Lett.*, 1997, 45, 35–40.
50. M. Breugst, R. Grée, K.N. Houk, Synergistic effects between Lewis and Brønsted Acids: Application to the Prins Cyclization, *J. Org. Chem.*, 2013, 78, 9892–9897.
51. A. Rauk, T.S. Sorensen, P. von Ragué Schleyer, Tertiary cyclohexylcations. Definitive evidence for the existence of isomeric structures (hyperconjomers), *J. Chem. Soc., Perkin Trans.*, 2001, 2, 869–874.
52. R.W. Alder, J.N. Harvey, M.T. Oabley, Aromatic 4-tetrahydropyranyl and 4-quinuclidinyl Cations. Linking Prins with cope and grob, *J. Am. Chem. Soc.*, 2002, 124, 4960–4961.
53. I. Il'ina, E. Morozova, A. Pavlova, D. Korchagina, T. Tolstikova, K. Volcho, N. Salakhutdinov, Synthesis and analgesic activity of aliphatic ketones-derived chiral hexahydro-2*H*-chromenes, *Med. Chem. Res.*, 2020, 29, 738–747.